

CHAPTER 39

Wave Velocity Field Measurements over a Submerged Breakwater.

Marco Petti,¹ Paul A. Quinn,² Gianfranco Liberatore³ & William J. Easson⁴

Abstract

The main focus of the experiment was to observe and measure large-scale vortices generated by breaking waves over a submerged breakwater. These flow structures are important in sediment transport due to their ability to trap sediment particles negating their normal settling velocity. The technique of Particle Image Velocimetry (PIV) was used to measure the spatial distribution of velocities at an instant; an approach which is essential for measuring coherent structures in the flow. Experiments were conducted in the 50m flume at The University of Florence which was fitted with a 1:100 beach, wave elevations, as well as velocity fields, were measured.

The paper deals with the experimental details and a display of the velocity and vorticity maps obtained using PIV.

Introduction

There is considerable interest in the use of submerged breakwaters for coastal protection purposes, but there is little information on the efficiency of such structures due to the poor knowledge of the local hydrodynamics. Consequently there are no analytical or numerical models (Kobayashi & Wurjanto, 89) which can fully describe the processes involved, and so experimental data is still valuable (Arhens, 89, Van der Meer, 90, Petti & Ruol, 91, 92). This study attempts to examine the velocity fields of waves breaking over submerged breakwaters, paying particular attention to the formation of large scale vortices formed by the breaking waves. These play a major part in sediment transport because sediment

¹Lecturer, Department of Civil Engineering, The University of Florence, Via di S. Marta, 3, I-50139 Florence, Italy.

²Research Associate, Fluid Dynamics Unit, Dept. of Physics & Astronomy, The University of Edinburgh, Edinburgh, EH9 3JZ, UK.

³Professor, University of Udine, Via Cotonificio, 114, 33100 Udine, Italy.

⁴Senior Lecturer, Department of Mechanical Engineering, The University of Edinburgh, Edinburgh, EH9 3JL, U.K.

particles can become trapped in vortices thereby losing their normal settling rates (Nielsen, 92, 94). Consequently how far these vortices travel and the time they take to decay is of significant interest. A further aspect to consider is the effect localised scour, due to large scale vortices, has on the stability of the structure. This paper concentrates on the experiments carried out and the initial results found, which are presented in the form of velocity and vorticity maps.

It is the technique of Particle Image Velocimetry (PIV) which is possibly the most novel aspect of this work; as it provides a spatial distribution of velocities at an instant it is ideal for measuring coherent structures. Previous experiments have used point measuring systems such as directional micro-propellers (Petti & Ruol, 1992) or electromagnetic velocimeters (Mizutani et al, 1992). This approach has the drawback that as only a time history of the wave velocity is obtained at a single point, coherent structures in the flow, such as large scale vortices, tend to get averaged out.

Particle Image Velocimetry (PIV)

A review of PIV is given by Adrian (1991) and an introduction to the process in a coastal engineering context is given by Greated et al (1992). Further references to work using PIV in this publication include Quinn et al (1994) and Earnshaw et al (1994). In order to avoid duplication I refer you to those papers for a brief overview of the processes involved.

The only additional point relating to these experiments was that the technique of image shifting was used (Bruce et al, 1992, Earnshaw et al, 1994). Without going into detail this allows us to measure zero and near-zero velocities and resolves the 180° directional ambiguity inherent with the autocorrelation method of PIV analysis; it is analogous to frequency shifting in Laser Doppler Anemometry (LDA).

Experiments

Experiments were carried out in the 50m flume at The University of Florence, which was fitted with a 1:100 sloping beach. For this study a submerged breakwater was installed about 26m from the wave maker and 22m from the foot of the beach. The breakwater was constructed of perspex with an Aluminium support structure and was 13.6cm high and 26 cm wide at the top, with an offshore facing slope of 1:3.5 and a shoreward facing slope of 1:1.5. The wave flume is shown in Figure 1 and the positions of the breakwater, PIV measurement section and wave gauges are indicated.

PIV was used to measure the velocity fields and a set of 16 parallel-wire resistance-type wave gauges were used to measure the surface elevations of the waves. The 15W Argon ion laser, PIV illumination system and photographic equipment were brought over from The University of Edinburgh for this collaborative study. The laser light sheet required for PIV has to be introduced into the

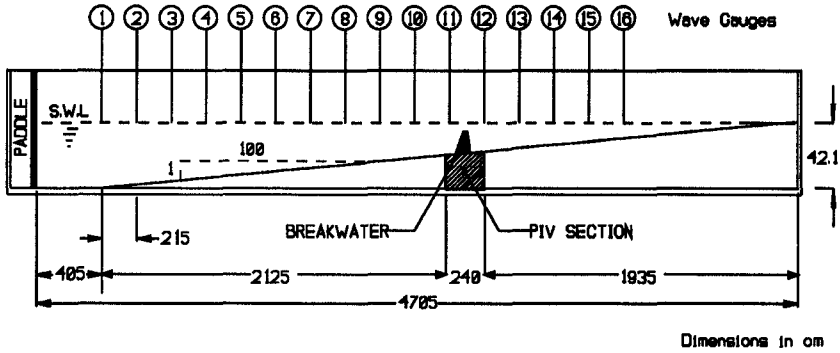


Figure 1: The Wave Flume at The University of Florence.

Test No.	Period, T_0 (s)	Wave Height, H_0 (m)	Ursell No.
1	2	0.10	19.2
2	3	0.10	47.0
3	4	0.14	89.3

Table 1: Wave Parameters

water from below the beach surface. As the bottom of the flume is not made of glass, a special section of the beach had to be built. This allowed the laser sheet in through the side of the flume, below the level of the beach and reflected it off an underwater mirror vertically up through a transparent strip in the beach into the flow. This is shown in Figure 2.

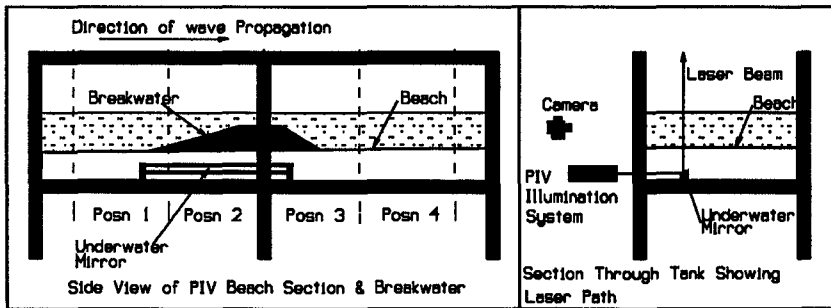


Figure 2: The PIV Beach Section

Three regular waves were used whose parameters are shown in Table 1. These

were chosen to break before, over and behind the structure. The waves were generated by a absorbing piston-type wave maker, in a water depth of 0.42m. PIV measurements were made at four positions around the breakwater and four phases of each wave, were recorded at each position, the phases being separated by 90° .

Wave Gauge Results

Figure 3 shows typical surface elevation records from gauges 1, 3, 5 & 7 for the 3s wave; Figure 4 shows the same for gauges 9, 11, 13 & 15. There are a couple of points worth noting here, firstly that gauge No. 1 is in constant depth water ($h_0 = 0.42\text{m}$) and secondly that gauge No. 11 is just in front of the breakwater.

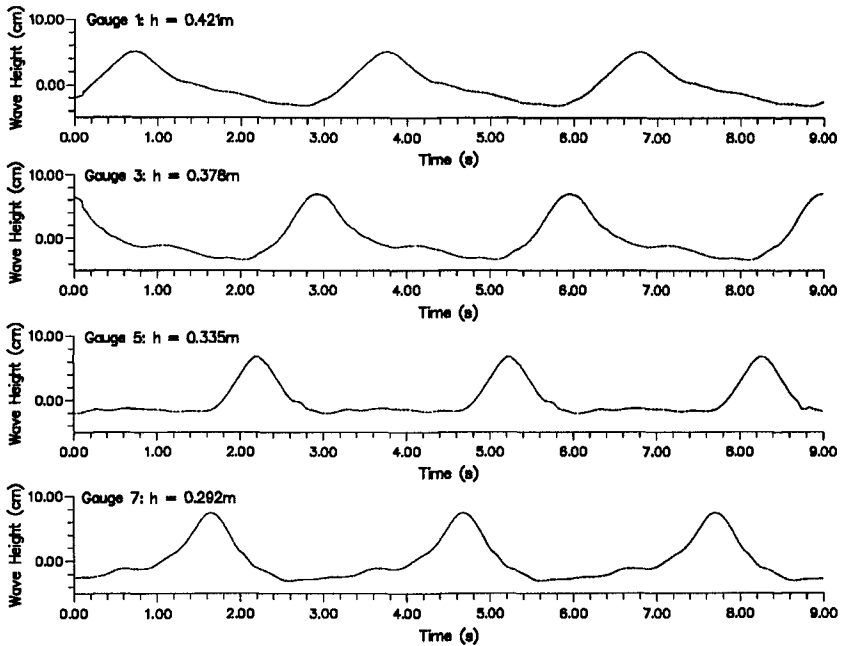
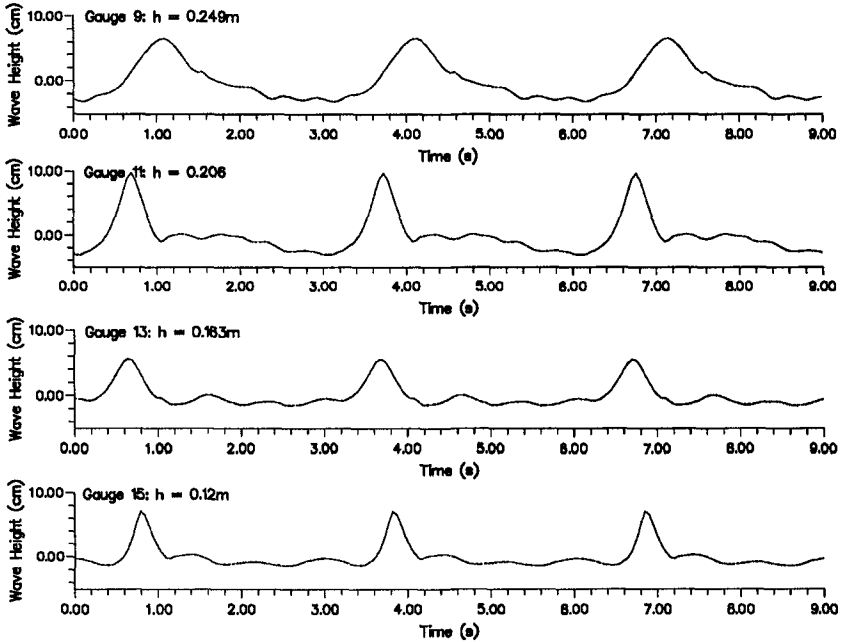


Figure 3: Wave Heights ($T = 3\text{s}$)

The first thing to notice from gauge 1 is that solely monochromatic waves are not being produced. There is definite evidence of a second wave being generated, and judging from the subsequent gauges this is a free wave, although it is at least of a much smaller amplitude than that of the main one. One can ascribe this generation of a free wave to the relatively high non-linearity of these waves. The Ursell numbers, calculated from Equation 1 are shown in Table 1; the values for the 3s & 4s waves being particularly high. It is perhaps not too surprising to see

Figure 4: Wave Heights ($T = 3s$)

this kind of instability from a wave maker trying to generate sinusoidal waves, Osborne & Petti (1994) give a more detailed description of this phenomenon.

$$U_0 = (H_0 L_0^2) / h_0^3 \quad (1)$$

Gauges 9 and 11 show significant reflected high-frequency waves, particularly in the troughs, with gauge 11 also showing the maximum wave elevation, of about 0.1m, due to its position just in front of the breakwater. In addition to this, one can also see (from Figures 3 & 4) how the phase celerity decreases as the waves approach the breakwater. Gauges 13 & 15 show diminished wave height and increased high frequency components following breaking, with evidence from gauge 15 of some frequency recombination as the wave crests have increased in height and sharpened in profile.

With the generation of a free wave and a measured reflection coefficient value of about 10%, there was a noticeable variation of wave heights at all the wave gauge positions. A zero-up-crossing significant wave height analysis from all 16 wave gauges was carried out and this gives a good indication of the scatter in wave heights. This zero-crossing analysis is given for all three waves in Figure 5

Although there is some significant scatter of the wave heights one can see the general trend of increasing wave height towards the breakwater, located just

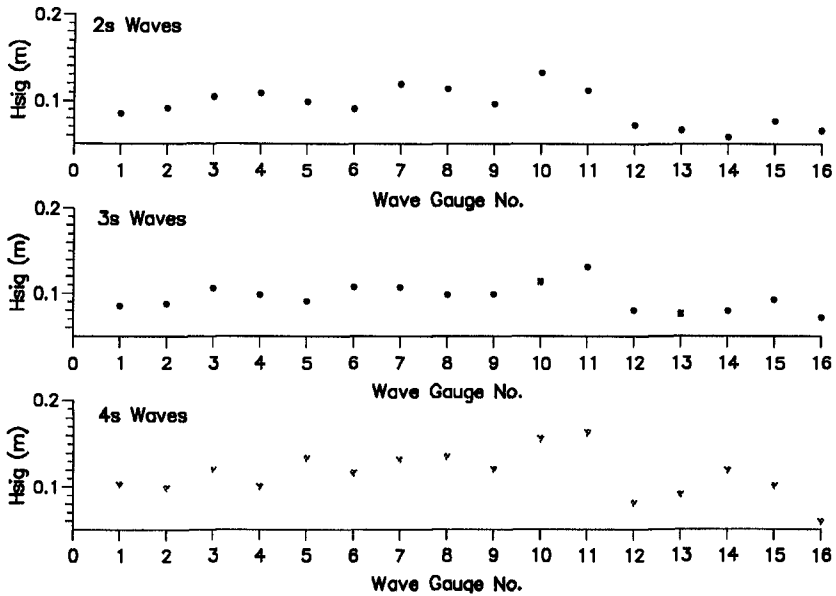


Figure 5: Zero up-crossing significant wave height distribution.

after gauge 11, and a decrease following breaking. The maximum waveheight was recorded at gauge number 10 for the 2s wave, this is due to the fact that the wave has already started to break by the time it reaches gauge 11. There is further evidence of post-breaking recombination of frequency components with the increase in significant wave height after the initial decrease due to breaking. This is particularly so for the 4s waves.

PIV Results

Due to the large number of measurements taken only a small set of the 48 velocity vector maps can be shown here. As the focus of the paper is the measurement of vortices generated by the breaking waves, only one example of a wave breaking on the front face of the breakwater is shown. The other results are presented, by means of velocity and vorticity maps, for the positions behind the breakwater. The convention of positive vorticity indicating an anti-clockwise rotation has been adopted throughout.

Figure 6 shows a 2s wave breaking on the front face of the breakwater. It is interesting to notice that the wave is breaking where the wave meets the fast flowing backwash, returning over the breakwater, and not at the top of the wave as one might expect. This formation of a localised bore on the structure gives

rise to small waves which travel in the offshore direction.

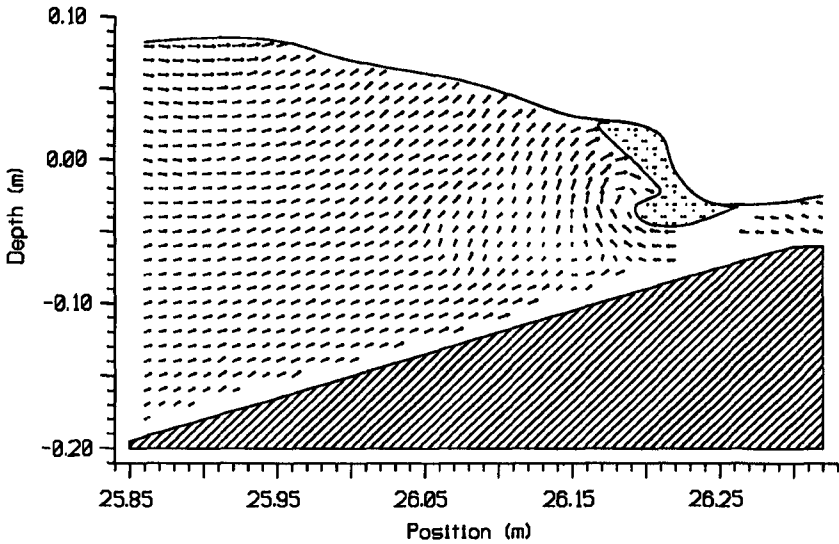


Figure 6: Vector map: 2s wave: Phase 4: Position 2.

Considering now the 3s wave, Figures 7, 9 & 11 show velocity maps for the first three phases at position three, with Figures 8, 10 & 12 showing the corresponding vorticity maps.

Phase 1 shows a positive vortex down near the bottom of the breakwater in an area particularly sensitive to scour, (Liberatore, 92) . Phase 2 shows a large region of negative vorticity near the surface to the right caused by the overturning of the wave that has just broken, sweeping upwards the positive vortex that was located near the foot of the structure in the previous phase. A small negative vortex is also being shed by the top corner of the breakwater. The third phase shows that the main negative vortex of the previous phase has reduced to a ring of smaller vortices and the positive vortex has now either dissipated or been carried back over the structure.

If we now look at position 4 (shorewards of position 3) for the 3s wave we can see from Figures 13 & 14 that at phase 4 there is still a significant negative vortex. This is most likely to have been generated by the previous wave and has, therefore, persisted for about 5s and moved about 0.55m from the rear of the breakwater.

Turning our attention now to the 4s waves, Figures 15 & 17 show velocity maps for phases 2 & 3 at position 3, with Figures 16 & 18 showing their corresponding vorticity maps.

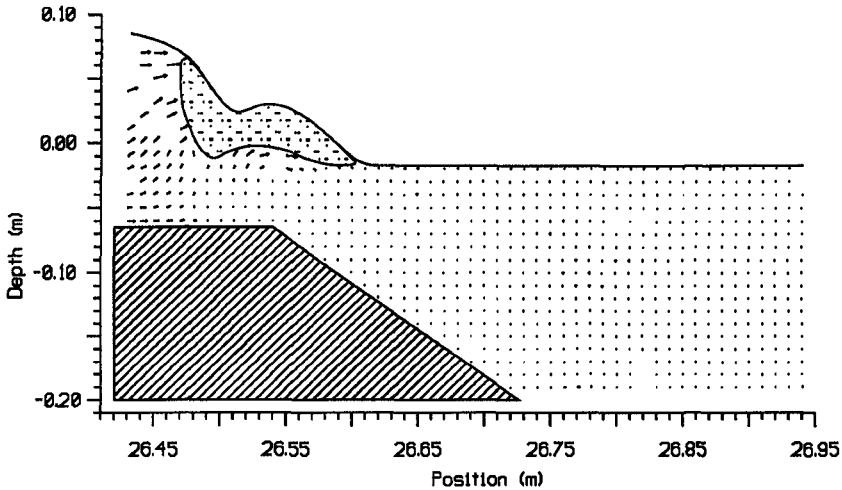


Figure 7: Vector map: 3s wave: Phase 1: Position 3.

Phase 2 shows negative vortices near the top right and on the top corner of the breakwater, the former being generated by the overturning breaker. There is a positive vortex above the rear toe of the structure in a similar position to the positive vortex shown at the same phase and position for the 3s wave. In phase 3, however, we can see that the large negative vortex has been swept into the next position and all that remains are two positive vortices near the bed and surface and a positive vortex being generated at the top corner of the structure as the flow returns back over the breakwater.

Moving on to the final position, Figure 19 shows the velocity maps for phase 2 again and Figure 21 shows the same for phase 4. Figures 20 & 22 show their vorticity maps, respectively. Phase 2 occurs just after the wave has broken and there is still some aeration of the flow near the surface, particularly near the centre of the figure. It has the greatest magnitude of vorticity values of any of the waves, with large negative vortices near the surface on the right of Figure 20 and near the bed on the left. Two phases later we can see that both negative vortices have persisted with the main one, centred about 27.09m in Figure 22 and the second one located on the left hand side of the flow.

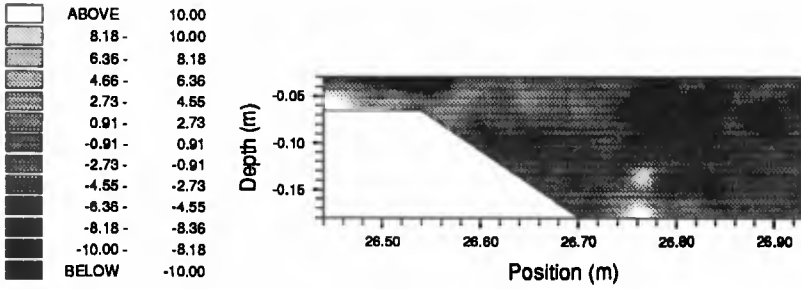


Figure 8: Vorticity map: 3s wave: Phase 1: Position 3.

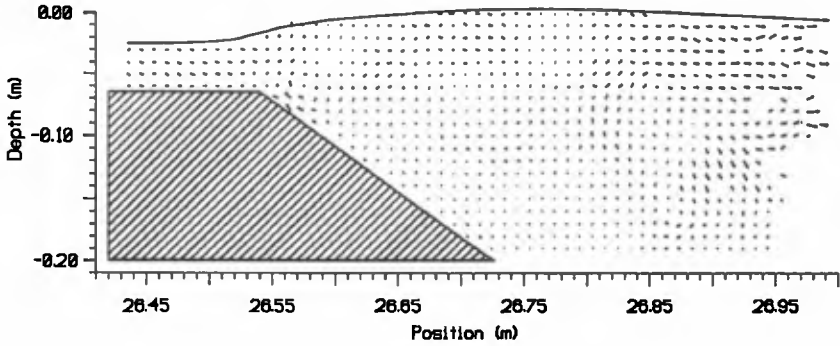


Figure 9: Vector map: 3s wave: Phase 2: Position 3.

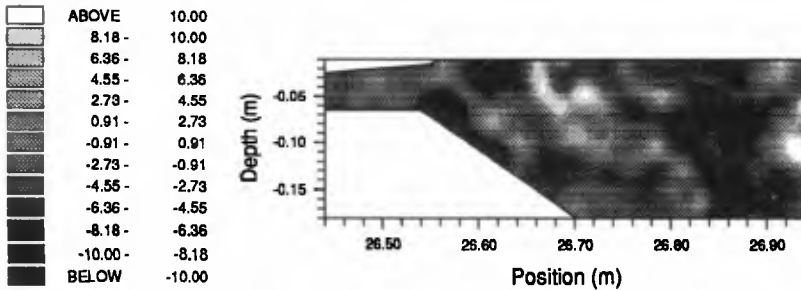


Figure 10: Vorticity map: 3s wave: Phase 2: Position 3.

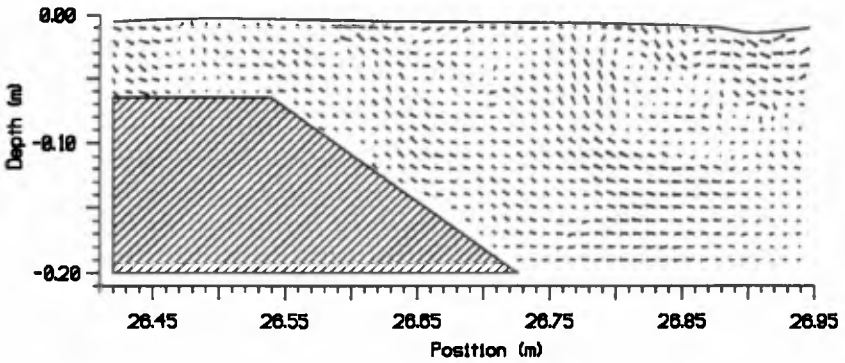


Figure 11: Vector map: 3s wave: Phase 3: Position 3.

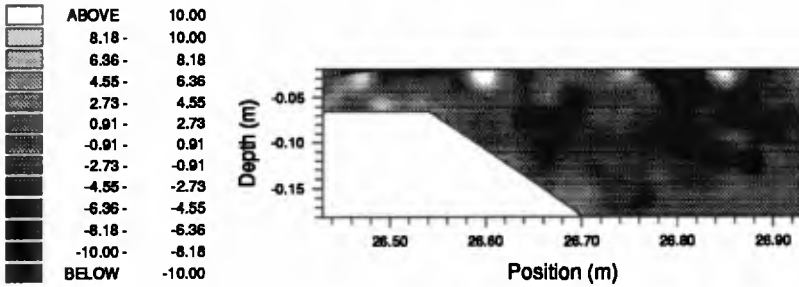


Figure 12: Vorticity map: 3s wave: Phase 3: Position 3.

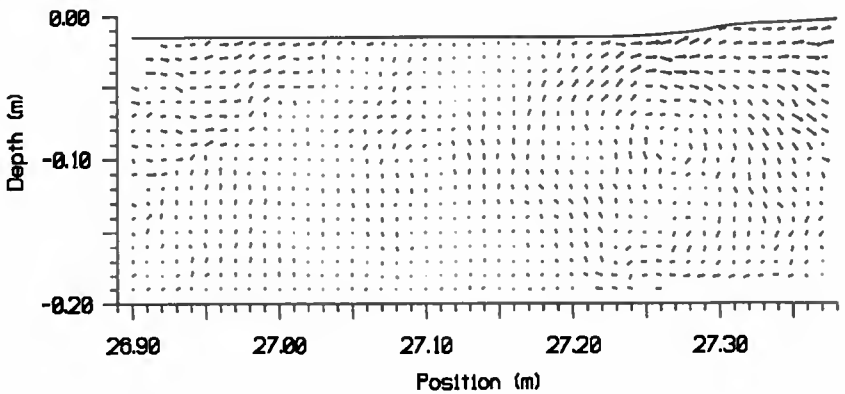


Figure 13: Vector map: 3s wave: Phase 4: Position 4.

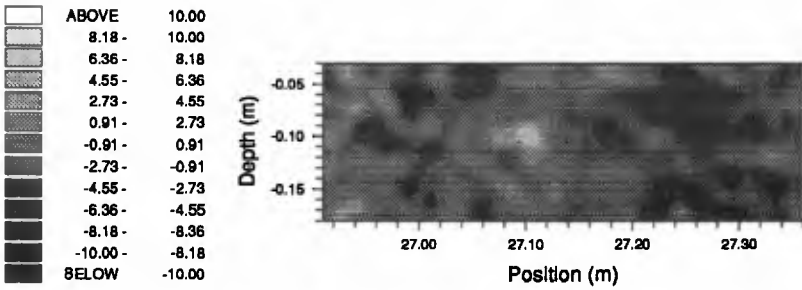


Figure 14: Vorticity map: 3s wave: Phase 4: Position 4.

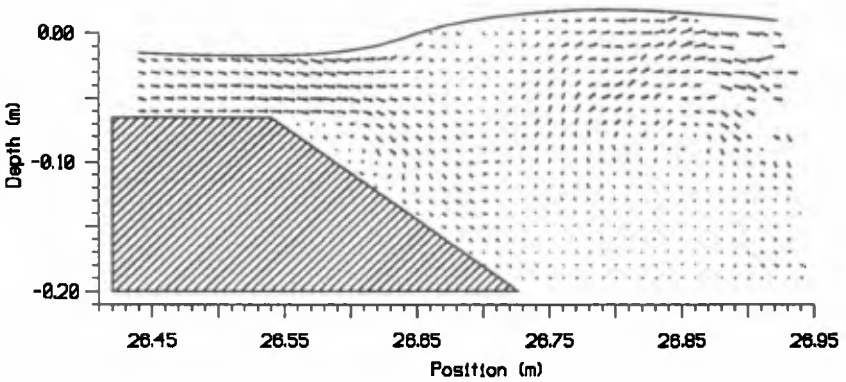


Figure 15: Vector map: 4s wave: Phase 2: Position 3.

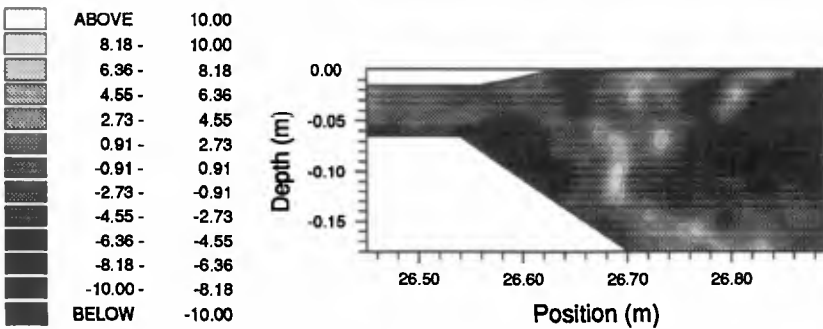


Figure 16: Vorticity map: 4s wave: Phase 2: Position 3.

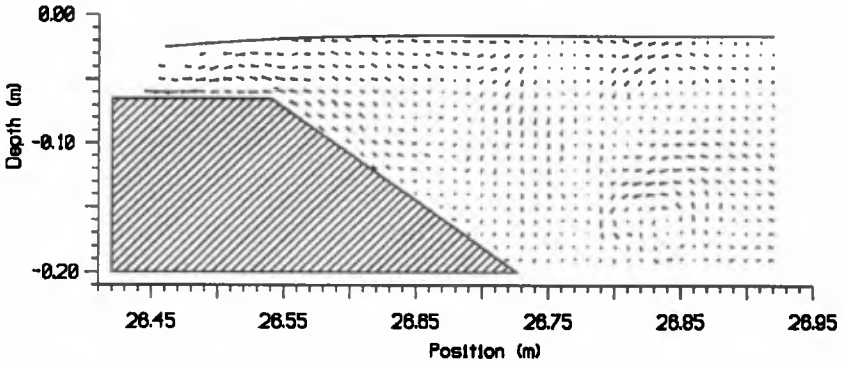


Figure 17: Vector map: 4s wave: Phase 3: Position 3.

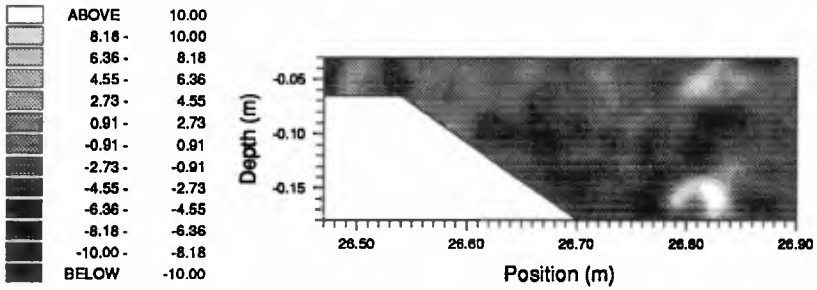


Figure 18: Vorticity map: 4s wave: Phase 3: Position 3.

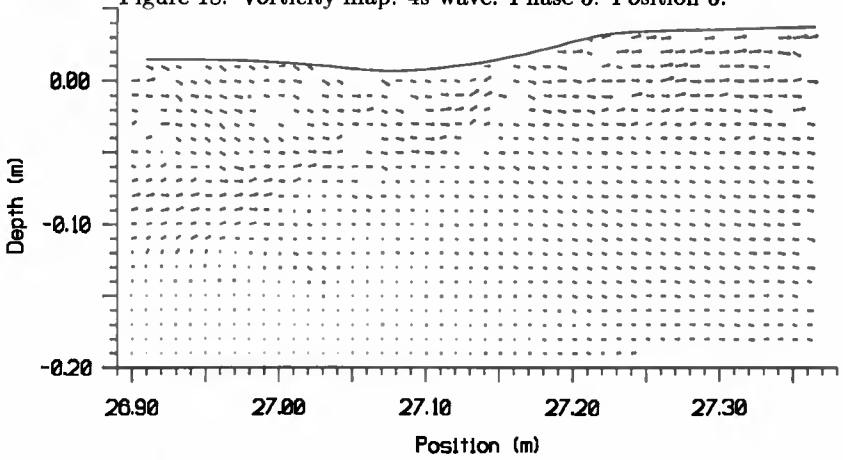


Figure 19: Vector map: 4s wave: Phase 2: Position 4.

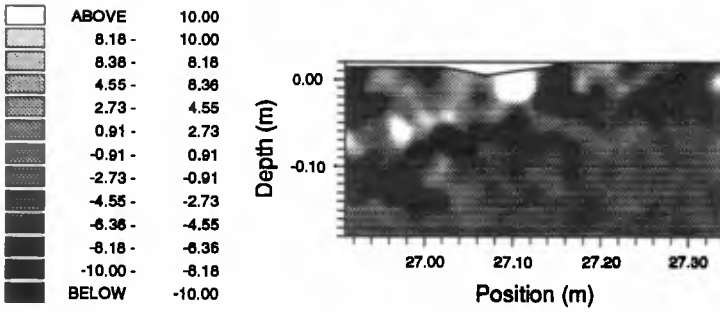


Figure 20: Vorticity map: 4s wave: Phase 2: Position 4.

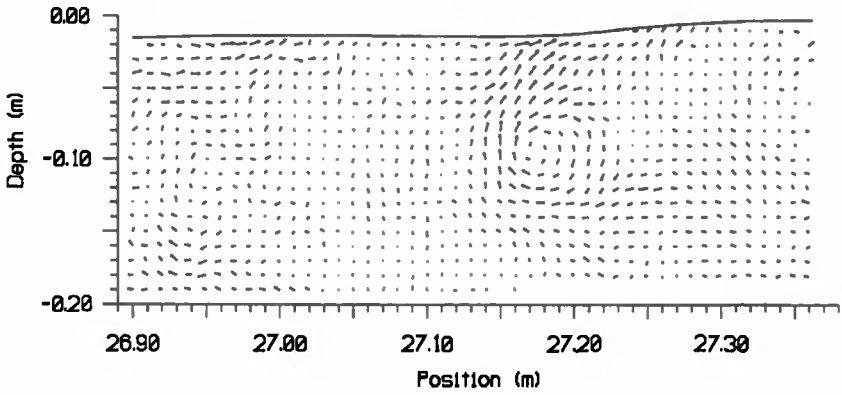


Figure 21: Vector map: 4s wave: Phase 4: Position 4.

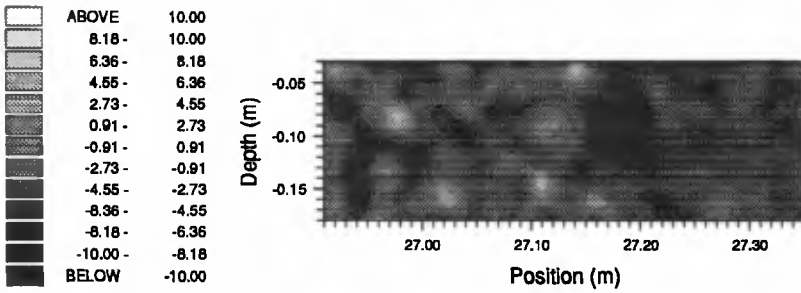


Figure 22: Vorticity map: 4s wave: Phase 4: Position 4.

Conclusions

The main focus of this study is to demonstrate the scale and significance of large scale vortices generated by waves breaking over a submerged breakwater. The ability to do this lies in the use of PIV as the measurement system, due to the fact that these flow structures are only measurable with a technique which records the spatial distribution of velocities at an instant. The detail of these measurements is apparent and a thorough analysis of the data is now called for. However, one can get an initial impression, from the results presented (eg. Figures 7-10 showing phases 1 & 2 of the 3s waves at position 3), of the importance of including vortex generation and interaction in the formulation of sediment transport numerical models. One such model is the Discrete Vortex Model described in Pedersen et al, 1992.

Acknowledgements

This work was undertaken as part of the MAST G8-M Coastal Morphodynamics research programme. It was funded by the Commission of the European Communities Directorate General for Science, Research and Development under contract N°. EC MAST-II OCT 92 0027; their support is greatly appreciated.

The authors also wish to extend their gratitude to the technicians, Mauro Gioli, Muzio Mascherini and Frank Morris, who played an essential role in conducting the experiments in Italy with such a tight time limit.

References

- Adrian, R.J. (1991) *Particle Imaging Techniques for Experimental Fluid Dynamics*. Ann. Rev. Fluid Mechanics, 23:261-304.
- Arhens, R.J. (1991) *Stability of Reef Breakwaters*. J. Waterway, Port, Coastal and Ocean Engineering, ASCE, 1729-1738.
- Bruce, T. & Easson, W.J., (1992) *The Kinematics of Wave Induced Flows Around Near-bed Pipelines*. Proc. 23rd Int. Conf. Coastal Eng. 229:2990-2998.
- Earnshaw, H.C., Bruce, T., Greated, C.A. & Easson, W.J. (1994) *PIV Measurements of Oscillatory Flow over a Rippled Bed*. Proc. 24th Int. Conf. Coastal Eng., Kobe, Japan.
- Greated, C.A., Skyner, D.J. and Bruce, T., (1992) *Particle Image Velocimetry (PIV) in the Coastal Engineering Laboratory*. Proc. 23rd Int. Conf. Coastal Eng. 15:212-225.
- Kobayashi, N. & Wurjanto, K. (1989) *Wave Transmission over Submerged Break-*

waters. J. Waterway, Port, Coastal and Ocean Eng., ASCE, (115) 5, 662-680.

Liberatore, G. (1992) *Detached Breakwaters and their use in Italy*. Proc. Short Course on Design and Reliability of Coastal Structures, 23rd Int. Conf. Coastal Eng.

Mizutani, N., Iwata, K., Rufin, T.M. and Kurata, K. (1992) *Laboratory Investigation on the Stability of a Spherical Armour Unit as a Submerged Breakwater*. Proc. 23rd Int. Conf. Coastal Eng. pp 1400-1413.

Nielsen, P. (1992) *Coastal Bottom Boundary Layers and Sediment Transport*. World Scientific, Singapore.

Nielsen, P. (1994) *Suspended Particle Motion in Coastal Flows*. Proc. 24th Int. Conf. Coastal Eng., Kobe, Japan.

Osborne, A.R. & Petti, M. (1994) *Laboratory Generated Shallow-Water Surface Waves: Analyses using the Periodic, Inverse Scattering Transform*. Physics of Fluids, Vol. 6, No. 5, 1727-1744.

Pedersen, C., Deigaard, R., Fredsøe, J. & Hansen, E.A. (1992) *Numerical Simulation of Sand in Plunging Breakers*. Proc. 23rd Int. Conf. Coastal Eng. pp 2344-2357.

Petti, M. and Ruol, P. (1991). *Experimental Studies on the Behaviour of Submerged Breakwaters*. Proc. 3rd Int. Conf. Coastal and Port Eng. in Developing Countries, 167-178.

Petti, M. and Ruol, P. (1992). *Laboratory Tests on the Interaction between Non-linear Long-waves and Submerged Breakwaters*. Proc. 23rd Int. Conf. Coastal Eng. pp 792-803.

Quinn, P.A., Petti, M., Drago, M. & Greated, C.A. (1994) *Velocity Field Measurements and Theoretical Comparisons for Non-Linear Waves on Mild Slopes*. Proc. 24th Int. Conf. Coastal Eng., Kobe, Japan.

Van der Meer, J.W. & Pilaczyk, K.W. (1990) *Stability of Low-Crested and Reef Breakwaters*. Proc. 22nd Int. Conf. Coastal Eng., ASCE, 1375-1388.